RSC Advances

PAPER

View Article Online
View Journal | View Issue

Cite this: *RSC Adv.*, 2015, **5**, 69243

Spray-on omniphobic ZnO coatings†

Nitin K. Neelakantan,[a] Patricia B. Weisensee,[b] John W. Overcash,[a] Eduardo J. Torrealba,[b] William P. King*[b] and Kenneth S. Suslick*[a]

Received 11th June 2015
Accepted 6th August 2015

DOI: 10.1039/c5ra11178a

www.rsc.org/advances

In recent years, the design of highly liquid-repellent surfaces has received great attention. Here, we report a facile method of creating a surface that repels both water and oils; using simple spray-coating, a hierarchically rough ZnO–PDMS composite can be applied to a variety of substrates that serves as a nanostructured surface for further modification. We applied an overcoating of either a fluoropolymer (Teflon AF) or perfluorodecyltrichlorosilane to fabricate low energy surfaces that repel water and oil for a variety of potential uses. The resultant surfaces are superomniphobic, have static contact angles of >140° for droplets of both liquids, and have low sliding angles for both water and oil droplets: <5° for water and <20° for oil.

Introduction

Liquid-repellent surfaces have high promise to improve surface properties for a wide range of applications in diverse fields, such as self-cleaning fabrics, anti-fouling coatings, water–oil separation, desalination, and condensation heat exchangers.[1–8] Many draw inspiration from the Lotus plant,[9] whose microstructure provides a self-cleaning mechanism through tiny air pockets that prevent penetration by water, leading to a Cassie–Baxter state[10] characterized by low contact angle hysteresis (CAH) and low tilt angle (*i.e.*, roll-off or sliding angle). Synthetic surfaces that mimic the Lotus leaf[11–13] rely on hierarchical roughness to prevent wetting by water. Due to their low surface tension, most oils cannot form contact angles greater than 90° on flat surfaces or those with nano- and microstructures with positive or vertical slopes. Re-entrant structures with overhanging slopes are necessary to repel these kinds of liquids.[14–16] So-called 'superomniphobic' surfaces[17,18] repel both water and a variety of oils and other low surface-tension liquids and are characterized by high droplet mobility. Superomniphobic surfaces have been prepared by a number of methods: *e.g.*, lithographically patterned roughness, low surface energy coatings, metal oxide nanoparticle coatings, electrodeposition, and electrospun textured polymers.[19–27]

A key challenge for omniphobic surfaces is facile and scalable fabrication. Many of the methods used to fabricate omniphobic surfaces are tedious, multi-step procedures requiring specialty equipment and chemicals, and in many cases are simply too expensive to implement at scale. In the same vein, silicon wafers are commonly used as the substrate,[16,18,21] but these are not often relevant to industrial or real-world applications. There is a need for methods that are compatible with a wide variety of substrate materials, including glass, metals and polymers. Of the many ways for making omniphobic surfaces, spray-coating would have significant advantages: an aerosol from a precursor solution containing the necessary chemical components can coat a surface evenly regardless of its dimensions, geometry, or substrate material. Spray-coating is also inexpensive and easily scaled-up. Nanoparticle zinc oxide (ZnO) is a suitable precursor, as it is non-toxic, commercially available, and intrinsically textured.

Using a polydimethylsiloxane (PDMS) binder, we report a simple method of fabricating a hierarchically roughened surface with intrinsic re-entrant structures based on a simple spray-coating that can be easily modified with a low surface-energy overcoating (Fig. 1). Qualitative relationships between the surface chemistry, surface roughness, and wettability for various ZnO : PDMS mass ratios and surface coatings are presented. Given the interest in making superomniphobic surfaces that favor drop-wise condensation over film-wise condensation and thus improve the efficiency of condensers, we have examined quantitatively the wetting behavior of these surfaces with both water and a common refrigeration lubricant (RL). To that end, we have characterized the performance of these surfaces by measuring the static contact angles (SCA) and sliding angles (α) of water (surface tension = 72.6 mN m^{-1}) and RL-68H (from Emkarate Corp., surface tension = 27.7 mN m^{-1}).[28] RLs are generally polyol esters miscible with hydrofluorocarbon (HFC) refrigerants that cycle through a refrigerator and keep all moving parts properly lubricated. The goal of the present work is to prevent film formation of RL on refrigeration piping and condenser surfaces as a first step towards designing coatings

[a]*School of Chemical Sciences, University of Illinois, Urbana-Champaign, Urbana, Illinois, 61801, USA. E-mail: ksuslick@illinois.edu*

[b]*Department of Mechanical Science and Engineering, University of Illinois, Urbana-Champaign, Urbana, Illinois, 61801, USA. E-mail: wpk@illinois.edu*

† Electronic supplementary information (ESI) available: Additional table, image, videos, IR spectra, X-ray photoelectron spectroscopy measurements (XPS). See DOI: 10.1039/c5ra11178a

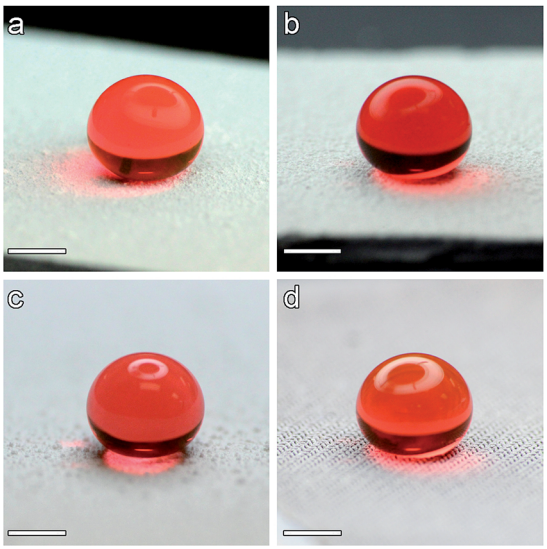

Fig. 1 Photographs of a water droplet (containing red dye) on spray coated surfaces of (a) aluminium, (b) silicon wafer, (c) cellulose filter paper and (d) copper mesh. All surfaces were spray-coated with a 2 : 1 solution of ZnO : PDMS. Scale bars represent 1 mm.

that could improve the performance of heat transfer equipment.

Experimental

Materials

Four materials were tested as substrates for the omniphobic coatings. Silicon wafers (150 mm diameter, 675 μm thick, type P, ⟨100⟩) were purchased from Ted Pella, Inc. and cut into 8 × 10 mm pieces. Other substrates examined include stock aluminium sheet (alloy 6061, 0.063″, McMaster-Carr, 12 × 25 mm), copper wire mesh (wire diameter 50 μm, mesh opening 75 μm, TWP Inc., 8 × 10 mm) and cellulose filter paper (qualitative grade, Whatman #1001, 70 mm diameter). Zinc oxide powder (NanoGard), particle diameter 40–100 nm, was used as received from Alfa Aesar. Sylgard 182 (Dow Corning), perfluorodecyltrichlorosilane (Gelest), and hexanes (Fisher Scientific) were used as received. RL-68H (Emkarate), Teflon AF 1600 (DuPont) and Fluorinert FC-770 (3M) were used as received.

Solution preparation

First, a stock solution of 0.25 g Sylgard 182 (PDMS)/mL hexanes was prepared. In a scintillation vial, 0.5 g ZnO was added; this was the standard amount used in fabricating all samples. The stock PDMS solution was added to the ZnO at mass ratios of 1 : 2, 1 : 1 and 2 : 1 ZnO : PDMS, *i.e.*, 4 mL, 2 mL and 1 mL respectively. Hexane was added to these solutions until the final volumes were ~20 mL. Then, the solutions were manually agitated to disperse the ZnO and PDMS evenly. This process was expedited by the use of an ultrasonication bath when necessary. Higher ratios of ZnO : PDMS (*i.e.*, 3 : 1, 4 : 1) resulted in dispersions that were insufficiently stable to permit spray deposition.

Spray procedure

For spraying procedure, aerosols were produced using a Badger 250 airbrush attached to a compressed air tank. Substrates were placed on a hot plate set to the lowest heat setting to facilitate solvent evaporation during spraying. The airbrush outlet is roughly 0.5 mm in diameter, and the air pressure used for spraying was 20 psi, corresponding to a flow rate of ~10 mL min^{-1}. The airbrush was held 15–20 cm from the substrate to ensure complete coverage and avoid any pooling of liquid on the surface. Coated samples were then cured in a Lindberg/Blue M programmable oven at 70 °C for 24 hours.

Teflon coating

After samples were removed from oven and cooled, a 5 : 1 v/v solution of Fluorinert FC-770 to Teflon AF was prepared. The amount necessary per sample is 100 μL FC-770 to 20 μL Teflon AF. Samples were dipped in a petri dish of the Teflon solution for 10–20 seconds so that the entire surface was coated. They were then placed in an oven and cured according to the manufacturer's instructions: 105 °C for 5 min, ramped over 5 min to 160 °C and held for 5 min, ramped over 5 min to 330 °C and held for 15 min.

Fluorosilane deposition

Alternatively, a liquid-phase deposition method similar to one previously reported in the literature[29] was used to functionalize uncoated ZnO–PDMS surfaces with a commercial fluorosilane. Samples were placed in a vial with 20 mL of hexanes, and then cooled to −10 °C. 50 μL of perfluorodecyltrichlorosilane (FDTS) were then added, and the reaction proceeded for 24 hours at −10 °C. The samples were then dried and rinsed with ethanol to remove any unwanted byproducts.

Some samples were also pre-treated with oxygen plasma for 1 min at 70 W and immediately submerged in 10 mL of toluene in a scintillation vial; 50 μL of FDTS were then added and allowed to react for 1 hour at room temperature.

Characterization

Electron microscope images of Teflon-coated samples were taken using a JEOL 7000F and a Philips XL30 ESEM-FEG scanning electron microscope. Samples were sputter-coated with Au/Pt for 25 s (a thickness of 7–8 nm) prior to image acquisition. 3D images and roughness data were acquired using an Alicona Infinite Focus 3D microscope, also after coating to reduce the diffuse scattering of the white ZnO and to enhance the image quality. The lateral resolution was 2 μm and the vertical resolution was 100 nm. On each sample, the data from a projected area of 1.04 × 0.58 mm^2 was measured and analyzed with the internal software provided by Alicona for surface roughness. It is important to note that the 3D microscope's resolution is much larger than the average nanoparticle size, thus, the calculations for roughness and conclusions derived from these calculations pertain to differences in microstructure only and not in the underlying nanostructure.

A Canon T3i camera with a Sigma 70–300 mm lens and a Raynox DCR-150 macro lens was used to capture photographs of droplets on various surfaces.

For contact angle measurements, a KSV CAM200 goniometer was employed. Water contact angle measurements used a 15 μL droplet size, whereas oil droplets were 5 μL in volume, the smallest dispensable quantities from the goniometer's custom micropipette, respectively. Static contact angle (SCA) was measured immediately after droplet deposition. Measurements are an average based on 10 images of a sample (acquisition rate: 1 image per second), for 3 different samples of each type made. This was done to ensure consistency in the spraying method and reproducibility across samples. The sliding angles were measured on a ThorLabs Goniometer stage by placing the droplet on the sample and then slowly tilting the stage until the droplet started moving. The angle was recorded and the measurement repeated for a minimum of 4 times to determine sliding angles. The droplet volumes were similar to those reported above for contact angle measurements.

Results and discussion

Spray-coating is a simple and effective method of coating a substrate because it is inexpensive, easily scalable, and applicable to a variety of surfaces.[30] The versatility of this approach permits any number of treatments to be applied to a single type of roughened surface. The spraying procedure employed in these experiments used a range of ZnO to PDMS ratios in order to investigate the effects of roughness on the contact angles of water and the refrigeration lubricant, RL-68H. Nanoparticle ZnO was to confer roughness to the surface, and PDMS acted as a polymer binder and hydrophobic contact surface. As a control, contact angles were also measured on a flat silicon wafer sprayed with PDMS. Since the flat PDMS coated wafer is relatively smooth, changes in contact angle of the ZnO modified surfaces can be attributed purely to changes in roughness.

Our coating process can be applied to a wide variety of substrates, including flat silicon wafer, stock aluminium sheet, copper mesh, and cellulose filter paper. Silicon wafers are not an essential substrate, but were examined in detail in order to make comparisons to prior studies of omniphobic coatings.[16,18,21] As shown in Fig. 1, superhydrophobic behaviour is observed for all four substrates with the same ZnO nanoparticle/PDMS coating; videos emphasize the superhydrophobic properties of these substrates (ESI, Video S1 and S2†).

The effect of modifying the surface energy was investigated by comparing ZnO : PDMS surfaces on silicon wafers to fluorocarbon over-coated counterparts. By comparing the liquid contact angles, we can compare the effects of surface roughness to the effects of changes in surface energy due to the over-coating for substrates of comparable roughness. For such comparisons, Teflon AF and perfluorodecyltrichlorosilane (FDTS) were each deposited from the liquid-phase onto ZnO/PDMS surfaces. Although FDTS has a lower critical surface energy (γ_c) than Teflon AF (12 mN m^{-1} *vs.* 16 mN m^{-1}), it only reacts with surface hydroxyl groups, forming a siloxane bond. Because the density of surface hydroxyl groups on the ZnO is limited, there is a trade-off with FDTS between the density of the total surface coverage *vs.* a lower γ_c. To improve the surface coverage, we plasma-oxidized samples before silanization to maximize the number of hydroxyl groups available for bonding. Examination of the Teflon AF and the FDTS surfaces permits comparison between a non-covalent *vs.* covalent over-coating procedures in terms of contact angles and sliding angles.

One might be tempted to incorporate low surface energy fluorochemicals into the initial polymeric binder rather than apply them as a second overcoat. Such an approach has two problems: first, bulk incorporation of a fluorocarbon does not guarantee that the fluorocarbon is actually present on the exposed surface. Second, large loadings of fluorochemicals into the polymeric binder would be necessary and the resulting composite may be dispersible only in expensive fluorinated solvents.[31–33] In addition, excessive use of fluorocarbons in general can be problematic because many fluorochemicals are precursors to perfluorooctanoic acid, a known bioaccumulant.[34] By separating the spray-coating and top-coating steps, the fluorocarbon is inherently on the contact surface and the amount of fluorocarbons necessary to coat the surface is greatly reduced.

Sample characterization

Fig. 2a–f shows SEM images of all ratios of ZnO : PDMS without a Teflon AF coating. As the relative amount of PDMS decreases compared to ZnO, an increase in texturing, due to increasing exposure of ZnO nanoparticles, can clearly be seen (*e.g.*, Fig. 2a *vs.* Fig. 2b *vs.* Fig. 2c). At a 2 : 1 ratio of ZnO : PDMS (Fig. 2c and f), individual nanoparticles protrude from the PDMS film, and a hierarchical roughness is observed that can best be described as micro-scale ZnO/PDMS globules which themselves consist of nano-scale ZnO papules. These hierarchical structures (Fig. 2c, f, i and l) produce an intrinsic multi-scale roughness with characteristic re-entrant structures necessary for omniphobicity with high contact angles and low roll-off angles.[35]

The initial aerosol droplets from the airbrush, which are tens of microns in diameter, deposit on the smooth Si surface. As the solvent evaporates, the ZnO nanoparticles and uncured PDMS coalesce. The PDMS then forms crosslinks as it cures and the final coating is produced. The emergence of hierarchical structures in the coating derives from the very different scales of the initial aerosol droplets (tens of μm) *vs.* the agglomeration of the ZnO nanoparticles–polymer composite as solvent evaporates (tens of nm). The spray process results in the formation of micro-scale re-entrant cavities, as can be seen in Fig. 3a. A close-up of one of these cavities (Fig. 3b) shows micro-scale globules with individual ZnO nanoparticles protruding from them, revealing the hierarchical roughness.

Fig. 2g–l shows the same samples after they have been coated with Teflon AF, and oven-cured. The same trend is observed as for the non-over-coated samples: higher relative ratios of ZnO produce a more textured surface and give a hierarchical structure. Compared to the samples without Teflon coating, more nano-scale ZnO papules emerge at the surface and increase the surface roughness (*e.g.*, compare Fig. 2f *vs.* Fig. 2l). The high heat treatment necessary to cure the Teflon AF alter the topographical appearance of PDMS, as confirmed by separate heat treatment of non-fluorinated samples.

Fig. 4 shows a 3D micrograph with a colored *z*-gradient of a Teflon AF coated 2 : 1 ZnO : PDMS surface, with an

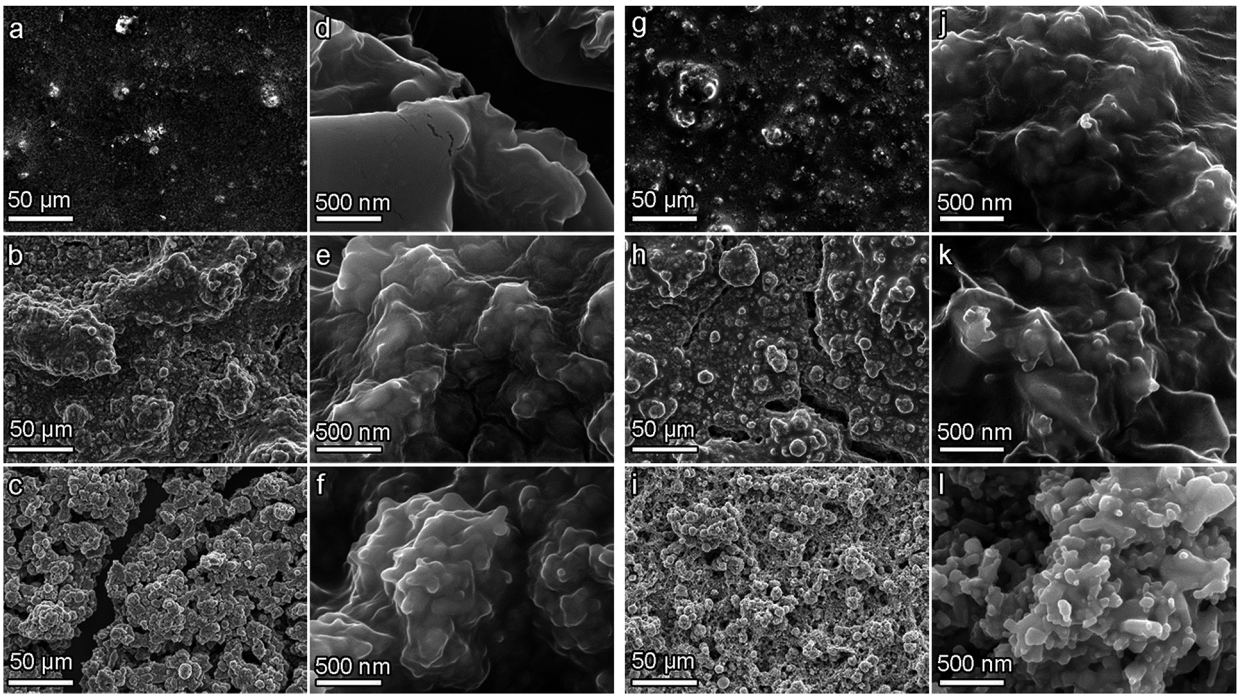

Fig. 2 SEM images of spray coatings of ZnO : PDMS at ratios of 1 : 2 (a and d), 1 : 1 (b and e) and 2 : 1 (c and f). Note the texturing at both the micro- and nano-scale. SEM images of spray coatings of ZnO : PDMS with a top-coating of Teflon AF at ratios of 1 : 2 (g and j), 1 : 1 (h and k) and 2 : 1 (i and l).

accompanying SEM images of the same sample section with a projected area of 1.04 mm × 0.58 mm and a detailed view from the center of the section (other 3D micrographs are provided in ESI Fig. S1a–e†). Peaks and valleys ranging from 30–200 μm are formed by the spray procedure contributing to the micro-scale roughness of the surfaces. The SEM images reveal additional nano-scale roughness that cannot be captured by the InfiniteFocus optical microscope. The *z*-gradient mapping allows for a qualitative comparison of surface roughness between the different ZnO : PDMS mass ratios and over-coating procedures. Table S1† lists the characteristic roughness parameters for all the samples under study.

We are not limited to flat surfaces in our coating process. The spray deposition can be used to effectively coat complex textured surfaces. For example, the coating of a copper mesh is shown in Fig. 5. The ZnO/PDMS coating forms the same hierarchically roughened structures discussed earlier (*i.e.* microglobules of ZnO and PDMS on Si wafer). Similar structures are observed using the spray coating process on stock aluminium and cellulose filter paper as well (Fig. 1).

Contact angle measurements

Table 1 shows the static contact angles of water and RL-68H the samples without Teflon AF coating. The 'PDMS on flat Si' sample, made by spraying a 25 mg mL^{-1} solution of PDMS onto a silicon wafer, acted as a flat reference sample with a similar surface chemistry as the samples with nanoparticles to study the effect of surface roughness on the contact angles. PDMS is intrinsically hydrophobic (surface energy = ~22 mN m^{-1}),[36] which leads to a SCA for water of 105°. RL-68H completely wets the surface. As the roughness of the samples increases, so does the water contact angle. In all cases, the de-wetting of water is improved by the spray-coating procedure when compared to the flat reference sample. On the 1 : 1 and 2 : 1 ZnO : PDMS, water contact angles of over >150° are achieved, indicating that the surfaces are highly hydrophobic, even without a fluorinated over-coating. The droplets are in the non-wetting Cassie–Baxter state.[37]

It is interesting to note that a non-zero contact angle for the refrigeration lubricant is obtained for a 1 : 1 ratio, yet the surfaces are completely wetted for the 2 : 1 and 1 : 2 ratios. This can be ascribed to a balance between the low surface energy from the PDMS (which would favor a lower ratio of ZnO to PDMS) *versus* the surface roughness from ZnO (which would favor a higher ratio). Interestingly, the 1 : 1 ZnO : PDMS surfaces have a higher micro-scale roughness than either the 2 : 1 or 1 : 2 mixtures (Table S1†). At either extreme, there is either not enough roughness and re-entrant structure (1 : 2) or not enough PDMS (2 : 1) to sustain droplet formation. Additionally, it is known that PDMS swells in the presence of many hydrocarbons,[38] which could explain the RL's affinity for the surface and the wetting at the low nanoparticle concentration.

Table 2 shows contact angles for Teflon-coated and fluorosilane-coated samples. The static contact angles on a smooth reference sample coated with Teflon AF, the contact angles are 120° for water and 75° for the lubrication oil. At a 1 : 2 ratio of ZnO : PDMS, the contact angles are almost identical to those of the smooth reference sample (*i.e.*, Teflon coated Si wafer), confirming that roughness is minimal. Water contact

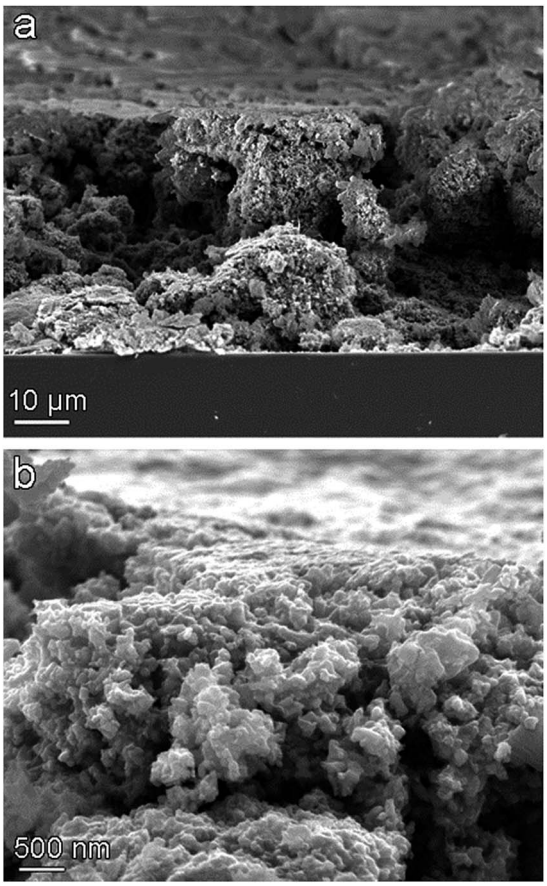

Fig. 3 Cross-sectional SEM of a 2 : 1 ZnO : PDMS spray-coated silicon wafer. (a) Cavities are formed by the spraying process showing re-entrant curvature. (b) Close-up of such a cavity.

angles on the 1 : 1 and 2 : 1 samples are similar to those without the Teflon AF coating. Unlike on the non-fluorinated samples, RL-68H contact angles increase dramatically with increasing ZnO : PDMS ratios, reaching a SCA > 135° at the 2 : 1 ratio. By changing the overcoating to FDTS, the contact angles of RL-68H were increased even more.

Surprisingly, RL-68H displayed higher contact angles than water on FDTS overcoated samples (Table 2) despite the fact that the oil has a much lower surface tension. This may be due to hydroxyl groups present on the surface, which can be a result of partially hydrolyzed silanes (*i.e.* silanol (Si–OH) formation). OH stretches are visible in the broad 3500 band in the IR of this sample (ESI Fig. S2c†) for surfaces not plasma treated. Polar OH groups would raise the surface tension of the surface, but are balanced by the very low surface energy of the FDTS itself. It is very important to note, however, that polar groups tend to raise the *polar* component of surface tension as opposed to the dispersive (van der Waals) component. Non-polar liquids, such as oils, tend to interact with the dispersive component, whereas polar liquids, such as water or milk, interact strongly with polar groups *via* hydrogen bonding.[39] Recent work has even exploited this idea by infusing ionic liquids into surfaces that can repel oils.[40] Plasma oxidation before silanization ensures that the silane reacts fully with the surface (rather than with itself,

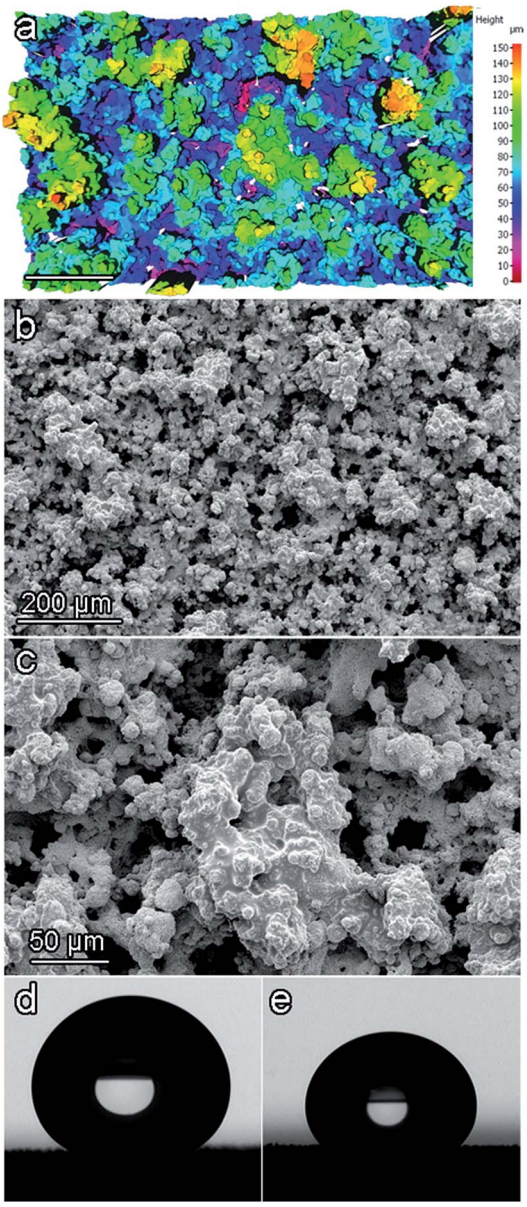

Fig. 4 (a) 3D microscopic image of a 2 : 1 ZnO : PDMS surface coated with Teflon taken on an InfiniteFocus 3D microscope; the area scanned was 0.58 mm × 1.04 mm; the scale bar is 200 μm. (b) SEM image of the same area and (c) insert showing detailed micro- and nano-structures. Optical image of a (d) water droplet and (e) RL-68H droplet on the same surface.

leading to partial hydrolysis producing the surface silanol groups), and no OH stretches are observed in the plasma oxidized material (ESI Fig. S2c†). As a consequence, plasma treated samples show an increased density of the fluorocarbon over-coat (confirmed by XPS, see Table S2†) which results in a surface more hydrophobic and more oleophobic. Since RL-68H is more sensitive to the surface chemistry than water (compare Tables 1 and 2), the increase in fluorocarbon density has a higher impact on the oil's contact angles.

Table 3 presents the sliding angles of water and RL-68H droplets. Water droplets do not slide on surfaces that were sprayed at ratios of 1 : 2 ZnO : PDMS, with or without a Teflon

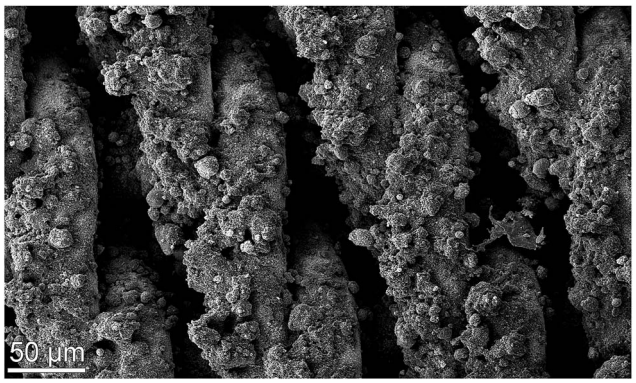

Fig. 5 SEM of a copper mesh spray coated with a 2 : 1 solution of ZnO : PDMS.

overcoat. The low roughness and the few extruding nanoparticles on these samples pin the three-phase contact line and act as barriers to the movement of the droplet.[41] At 1 : 1 and 2 : 1 ZnO : PDMS ratios, both uncoated and Teflon-coated surfaces have sliding angles of 5° or less for water droplets. These surfaces are thus superhydrophobic. FDTS-coated samples, however, have a sliding angle with water of 20°. This is consistent with only partial coverage of the surface with FDTS, as noted earlier. When the 2 : 1 ZnO : PDMS sample is plasma-oxidized prior to silanization with FDTS, however, the water sliding angle achieve again sliding angles of 5°. RL-68H droplets were pinned (*i.e.*, even when the surface was tilted by 90°, the droplet was immobile) on all surfaces except on the plasma-oxidized, silanized sample. Oil droplets slide off easily at an angle of 17°. RL-68H droplets moving across this surface leave no oily stains behind, indicating a highly de-wetted state (Video S3†).

To provide further information on mechanism and scope of the surface interactions, we have also examined our surface interactions with milk, whose surface tension[42] (γ = 54 mN m^{-1}) is intermediate between water and oil. Milk was used as an example of a more complex fluid and a good choice with which to show omniphobicity. Milk contains fats, proteins, and sugars, and importantly its morphology is a hydrophobic colloidal suspension in water. The results of surface contact angle measurements are shown in ESI Table S3† and are generally close to those of water.

Table 1 Static contact angles of water and RL-68H on ZnO : PDMS coatings

ZnO : PDMS ratio	Top coat	θ, H_2O (°)	θ, RL-68H (°)
PDMS on flat Si	—	105 ± 2	Wetted, ~0
1 : 2	—	119 ± 11	Wetted, ~0
1 : 1	—	155 ± 2	60 ± 4
2 : 1	—	152 ± 6	Wetted, ~0

Table 2 Static contact angles of water and RL-68H on ZnO : PDMS coatings with fluorinated overcoatings

ZnO : PDMS ratio	Top coat	θ, H_2O (°)	θ, RL-68H (°)
Flat Si	Teflon AF	120 ± 6	75 ± 3
1 : 2	Teflon AF	117 ± 3	79 ± 3
1 : 1	Teflon AF	156 ± 2	72 ± 4
2 : 1	Teflon AF	157 ± 2	137 ± 2
2 : 1	FDTS	126 ± 6	146 ± 5
2 : 1	FDTS, plasma-treated	144 ± 2	148 ± 2

Table 3 Sliding angles (α) of water and RL-68H on ZnO : PDMS coatings

ZnO : PDMS ratio	Top coat	α, H_2O (°)	α, RL-68H (°)
2 : 1	FDTS, plasma treated	5	17
2 : 1	FDTS	20	Pinned
2 : 1	Teflon AF	5	Pinned
2 : 1	None	2	Wetted
1 : 1	Teflon AF	5	Pinned
1 : 1	None	3	Pinned
1 : 2	Teflon AF	Pinned	Wetted
1 : 2	None	Pinned	Wetted

Previous publications report progress with omniphobic ZnO-based coatings,[29,32,43,44] as given in Table 4. Steele and coworkers pioneered the fabrication of an omniphobic surface based on a sprayable solution of nanoparticle ZnO with a perfluorinated methacrylic copolymer (PMC) dispersed in acetone.[43] When comparing contact angle data, they achieved results similar to ours but no sliding angle data was reported.

In subsequent work, however, Steele and coworkers noted that their PMC/ZnO solution cured in an uneven coating when applied to a micro-molded PDMS substrate and sometimes left hydrophilic regions on the surface.[44] This multistep process required (1) prior fabrication of micro-posts of PDMS, (2) followed by fluorosilane deposition, (3) modified with dispersion onto the surface of a surfactant solution containing nanoparticle ZnO, and (4) completed with a final treatment with fluorosilane deposition. The contact and sliding angle data for water droplets are similar to our data, but neither oils nor low surface-tension liquids were tested.

Perry and co-workers synthesized ZnO nanostructures using a chemical bath deposition on a silicon wafer, which was then functionalized either with a C_4F_8 plasma or by treatment with FDTS.[29] They achieved high contact angles and low sliding angles for water droplets and aqueous ethanol droplets; aqueous ethanol has significantly higher surface tensions than RL-68H and no tests were reported for alkanes, oils or other low surface-tension liquids.

Lastly, Campos *et al.* used fluoroalkyl-functionalized silica instead of ZnO nanoparticles in an ETP-600S fluoropolymer matrix to study the effect of the particle mass fraction on contact angles and sliding angles of water, diiodomethane, rapeseed oil and hexadecane.[32] Hexadecane (similar surface tension to RL-68H) showed similar contact angles as the oil in our study, however, the sliding angles were somewhat higher than that obtained in the present study. The present work improves upon both the fabrication of omniphobic surfaces as well as their application to oils.

Table 4 Literature reports of liquid-repellent nanoparticle and spray coatings

Omniphobic coating	Method of deposition	Liquids tested	Static contact angles (SCA)/sliding angles (α)
ZnO nanoparticles and fluorocarbon–methacrylate copolymer[40]	Sprayed onto glass slides	Water ($\gamma = 72.6$ mN m^{-1}) Hydraulic oil (γ = n.r.) Hexadecane ($\gamma = 27.5$ mN m^{-1})	SCA > 150° for all liquids; sliding angles not reported
ZnO nanoparticles with quaternary amine surfactant[41]	Sprayed onto micro-molded PDMS substrate, then functionalized with fluorosilanes	Water ($\gamma = 72.6$ mN m^{-1})	SCA > 150°, $\alpha < 2°$
ZnO nanostructures with fluorosilane[29]	Nanostructures made *via* chemical bath deposition onto silicon wafer	Water ($\gamma = 72.6$ mN m^{-1}) 30% aq. ethanol ($\gamma = 35$ mN m^{-1})	SCA ~ 160° SCA ~ 145°, $\alpha = 10°$
Fluoroalkyl-functionalized silica + 20 wt% added fluorocarbon[32]	Sprayed onto flat wafer	Water ($\gamma = 72.6$ mN m^{-1}) Diiodomethane ($\gamma = 50.8$ mN m^{-1}) Rapeseed oil ($\gamma = 35.5$ mN m^{-1}) Hexadecane ($\gamma = 27.5$ mN m^{-1})	SCA ~ 165°, $\alpha < 5°$ SCA ~ 151°, $\alpha < 5°$ SCA ~ 153°, α ~10° SCA ~ 150°, α ~ 25°
Current work: ZnO–PDMS + FDTS	Sprayed onto flat wafer	Water ($\gamma = 72.6$ mN m^{-1}) Milk, 1% fat ($\gamma = 54$ mN m^{-1}) RL-68H ($\gamma = 27.7$ mN m^{-1})	SCA ~ 144°, $\alpha < 5°$ SCA ~ 148°, $\alpha < 5°$ SCA ~ 148°, α ~ 17°

Liquid-repellent behavior of our surfaces is correlated first and foremost with surface energy, and then with surface roughness. This is corroborated by the data on our fluorinated overcoated surfaces: the FDTS-coated samples (which have lower surface energy) are more omniphobic than their Teflon-coated counterparts (which were on average, rougher, see ESI Table S1†). Surface energy correlates strongly with the amount of fluorocarbons present on the surface, as evidenced by the XPS elemental analysis (ESI Table S2†): our most omniphobic samples also have the highest fluorine content. The effect of surface roughness can be separated from the effects of surface energy in our non-overcoated ZnO : PDMS surfaces, where the actual composition of the surface is essentially unchanged and consists mostly of PDMS (confirmed by the XPS elemental analysis, ESI Table S2†). As the surface roughness increases (*i.e.*, from 1 : 2 to 1 : 1 to 2 : 1 ZnO : PDMS), liquid repellency increases.

Conclusions

In conclusion, we have developed a sprayable ZnO-PDMS composite that makes surfaces hydrophobic. In addition, an overcoating of Teflon AF or FDTS increases liquid repellency of the sprayed surfaces and renders them omniphobic. The low cost (ESI Table S4†), ease of use, and scalability of this procedure make it an attractive option for a variety of surfaces that would otherwise be difficult to coat. We report static contact angles of ~150° for water and the refrigeration oil RL-68H. Water droplet mobility is excellent on the superhydrophobic surfaces with a ratio of ZnO to PDMS of at least 1 : 1. Highest contact angles with the oil are achieved with a 2 : 1 ZnO : PDMS mixture. By functionalizing the surface with plasma oxidation and silanization, oil sliding angles as low as 17° were achieved. Future work aimed at promoting droplet condensation in refrigeration condensers, however, will need to focus on fabricating surfaces that repel liquids with even lower surface tensions.

Acknowledgements

Portions of this work were carried out in part at the Frederick Seitz Materials Research Laboratory, the Beckman Institute for Advanced Science and Technology, and the Micro- and Nano-Mechanical Systems Cleanrooms, UIUC. This research was supported by NSF DMR 1206355 and ONR N00014-12-1-0014. We gratefully acknowledge the assistance of Rick Haasch, who carried out XPS measurements on coated samples.

Notes and references

1 N. Miljkovic, R. Enright and E. N. Wang, *ACS Nano*, 2012, **6**, 1776–1785.
2 M. Nosonovsky and B. Bhushan, *Curr. Opin. Colloid Interface Sci.*, 2009, **14**, 270–280.
3 Z. Xue, S. Wang, L. Lin, L. Chen, M. Liu, L. Feng and L. Jiang, *Adv. Mater.*, 2011, **23**, 4270–4273.
4 J. Yang, Z. Zhang, X. Xu, X. Zhu, X. Men and X. Zhou, *J. Mater. Chem.*, 2012, **22**, 2834–2837.
5 I. Banerjee, R. C. Pangule and R. S. Kane, *Adv. Mater.*, 2011, **23**, 690–718.
6 C. Fang, J. E. Steinbrenner, F.-M. Wang and K. E. Goodson, *J. Micromech. Microeng.*, 2010, **20**, 045018.
7 A. Larbot, L. Gazagnes, S. Krajewski, M. Bukowska and W. Kujawski, *Desalination*, 2004, **168**, 367–372.
8 Y. Liu, J. Tang, R. Wang, H. Lu, L. Li, Y. Kong, K. Qi and J. Xin, *J. Mater. Chem.*, 2007, **17**, 1071–1078.
9 W. Barthlott and C. Neinhuis, *Planta*, 1997, **202**, 1–8.
10 A. Cassie and S. Baxter, *Trans. Faraday Soc.*, 1944, **40**, 546–551.
11 R. Fürstner, W. Barthlott, C. Neinhuis and P. Walzel, *Langmuir*, 2005, **21**, 956–961.
12 S. Nishimoto and B. Bhushan, *RSC Adv.*, 2013, **3**, 671–690.
13 T. Sun, L. Feng, X. Gao and L. Jiang, *Acc. Chem. Res.*, 2005, **38**, 644–652.

14 A. Tuteja, W. Choi, G. H. McKinley, R. E. Cohen and M. F. Rubner, *MRS Bull.*, 2008, **33**, 752–758.
15 D. Quéré, *Annu. Rev. Mater. Res.*, 2008, **38**, 71–99.
16 T. L. Liu and C. Kim, *Science*, 2014, **346**, 1096–1100.
17 A. Tuteja, W. Choi, M. Ma, J. M. Mabry, S. A. Mazzella, G. C. Rutledge, G. H. McKinley and R. E. Cohen, *Science*, 2007, **318**, 1618–1622.
18 A. Tuteja, W. Choi, J. M. Mabry, G. H. McKinley and R. E. Cohen, *Proc. Natl. Acad. Sci.*, 2008, **105**, 18200–18205.
19 T. Darmanin and F. Guittard, *J. Colloid Interface Sci.*, 2009, **335**, 146–149.
20 T. Darmanin and F. Guittard, *Soft Matter*, 2013, **9**, 1500–1505.
21 L. Cao, T. P. Price, M. Weiss and D. Gao, *Langmuir*, 2008, **24**, 1640–1643.
22 R. Dufour, M. Harnois, Y. Coffinier, V. Thomy, R. Boukherroub and V. Senez, *Langmuir*, 2010, **26**, 17242–17247.
23 K. Golovin, D. H. Lee, J. M. Mabry and A. Tuteja, *Angew. Chem., Int. Ed.*, 2013, **52**, 13007–13011.
24 A. Grigoryev, I. Tokarev, K. G. Kornev, I. Luzinov and S. Minko, *J. Am. Chem. Soc.*, 2012, **134**, 12916–12919.
25 H. Kim, K. Noh, C. Choi, J. Khamwannah, D. Villwock and S. Jin, *Langmuir*, 2011, **27**, 10191–10196.
26 S. P. Kobaku, A. K. Kota, D. H. Lee, J. M. Mabry and A. Tuteja, *Angew. Chem., Int. Ed.*, 2012, **51**, 10109–10113.
27 G. Soliveri, R. Annunziata, S. Ardizzone, G. Cappelletti and D. Meroni, *J. Phys. Chem. C*, 2012, **116**, 26405–26413.
28 M. A. Kedzierski and M. Gong, Effect of CuO nanolubricant on R134a pool boiling heat transfer with extensive measurement and analysis details, *Report NISTIR 7454*, National Institute of Standards and Technology, Gaithersburg, MD, 2007.
29 G. Perry, Y. Coffinier, V. Thomy and R. Boukherroub, *Langmuir*, 2012, **28**, 389–395.
30 A. Lefebvre, *Atomization and Sprays*, Taylor & Francis, New York, 1989.
31 S. Srinivasan, S. S. Chhatre, J. M. Mabry, R. E. Cohen and G. H. McKinley, *Polymer*, 2011, **52**, 3209–3218.
32 R. Campos, A. J. Guenthner, A. J. Meuler, A. Tuteja, R. E. Cohen, G. H. McKinley, T. S. Haddad and J. M. Mabry, *Langmuir*, 2012, **28**, 9834–9841.
33 J. M. Mabry, A. Vij, S. T. Iacono and B. D. Viers, *Angew. Chem., Int. Ed.*, 2008, **47**, 4137–4140.
34 R. Renner, *Environ. Sci. Technol.*, 2001, **35**, 154A–160A.
35 A. Marmur, *Langmuir*, 2008, **24**, 7573–7579.
36 M. K. Chaudhury and G. M. Whitesides, *Langmuir*, 1991, **7**, 1013–1025.
37 R. J. Vrancken, H. Kusumaatmaja, K. Hermans, A. M. Prenen, O. Pierre-Louis, C. W. Bastiaansen and D. J. Broer, *Langmuir*, 2009, **26**, 3335–3341.
38 J. N. Lee, C. Park and G. M. Whitesides, *Anal. Chem.*, 2003, **75**, 6544–6554.
39 F. M. Fowkes, *Ind. Eng. Chem.*, 1964, **56**, 40–52.
40 D. F. Miranda, C. Urata, B. Masheder, G. J. Dunderdale, M. Yagihashi and A. Hozumi, *APL Mater.*, 2014, **2**, 056108.
41 L. Barbieri, E. Wagner and P. Hoffmann, *Langmuir*, 2007, **23**, 1723–1734.
42 A. J. Bertsch, *J. Dairy Res.*, 1983, **50**, 259–267.
43 A. Steele, I. Bayer and E. Loth, *Nano Lett.*, 2009, **9**, 501–505.
44 A. Steele, I. Bayer, S. Moran, A. Cannon, W. P. King and E. Loth, *Thin Solid Films*, 2010, **518**, 5426–5431.

